Available online at www.sciencedirect.com
SCIENCE DIRECT®
International Journal of Thermal Sciences 43 (2004) 665–676
International Journal of Thermal Sciences
www.elsevier.com/locate/ijts

Simulation of heat and moisture transfer with phase change and mobile condensates in fibrous insulation

Xiaoyin Cheng, Jintu Fan *

Institute of Textiles and Clothing, Hong Kong Polytechnic University, Hung Hom, Kowloon, Hong Kong

Received 10 March 2003; accepted 14 November 2003

Available online 12 February 2004

Abstract

Numerical simulation has been reported on this paper for an improved model of coupled heat and moisture transfer with phase change and mobile condensates in fibrous insulation. The new model considers the moisture movement induced by the partial water vapor pressure, a super saturation state in condensing region as well as the dynamic moisture absorption of fibrous materials and the movement of liquid condensates. Based on simulation results, it has been found that moisture movement induced by the partial water vapor pressure, moisture diffusion, condensation, evaporation, and liquid water movement are the most important factors influencing the distribution of water content and heat loss. The results of the new model have been compared and found in good agreement with the experimental ones.

Keywords: Fibrous insulation; Phase change; Condensation; Moisture absorption; Heat and moisture transfer; Simulation

1. Introduction

Theoretical modeling of coupled heat and moisture transfer with phase change in fibrous insulation started with Henry's work in 1930s [1]. However, little further progress has been made until 1980s. Ogniewicz and Tien [2] are the first workers who have contributed the subject through theoretical modeling and numerical analysis, assuming heat is transported by conduction and convection and the condensate is in pendular state. The analysis was limited to a quasi steady state, viz. the temperature and vapor concentration remain unchanged with time before the condensates become mobile. Motakef and El-Masri [3] first considered the quasi steady-state corresponding to mobile condensate, under which the condensates diffuse towards the wet zone's boundaries as liquid and re-evaporates at these boundaries leaving the time-invariant temperature, vapor concentration and liquid content profiles. This theoretical model was later extended by Shapiro and Motakef [4] to analyze the unsteady heat and moisture transport processes and compared the analytical results with experimental ones under some very limited circumstances. This analysis was only valid when the time scale for the motion of the dry-wet boundary in porous media is much larger than the thermal diffusion time scale, which may however not be the case with frosting and small moisture accumulation [5].

Farnworth [6] presented the first dynamic model of coupled heat and moisture transfer with sorption and condensation. This model was rather simplified and only appropriate for multi-layered clothing as it was assumed that the temperature and moisture content in each clothing layer were uniform. Vafai and Sarkar [7] first modeled the transient heat and moisture transfer with condensation rigorously. For the first time, the interface between the dry and wet zones was found directly from the solution of the transient governing equations. In this work, the effects of boundary conditions, the Peclet and Lewis number on the condensation process is numerically analyzed. Later Vafai and Tien [8] extended the analysis to two-dimensional heat and mass transport accounting for phase change in a porous matrix. Tao et al. [5] first analyzed the frosting effect in an insulation slab by applying Vafai and Sarkar's model to the case with temperature below the triple point of water. Tao, Besant, and Rezkallah [9] have also for the first time considered the hygroscopic effects of insulation materials in the modeling. Murata [10] first considered the falling of condensate under gravity and built the phenomena into his steady-state model. Gibson and Charmchi [11,12] modeled the diffusion/convection of heat

* Corresponding author.
E-mail address: tcfanjt@inet.polyu.edu.hk (J. Fan).

1290-0729/$ – see front matter
doi:10.1016/j.ijthermalsci.2003.11.006

Nomenclature

C_a	water vapor concentration in the inter-fiber void space	$kg{\cdot}m^{-3}$
C_{ai}	moisture concentration at the boundaries (i.e., $i=0$: surface next to human body, $i=1$: surrounding air)	K
C_a^*	saturated water vapor concentration in the interfiber void space	$kg{\cdot}m^{-3}$
C_f	mean water vapor concentration in the fiber	$kg{\cdot}m^{-3}$
C'_f	volumetric moisture concentration in the fiber (it varies over the radius of the fibers)	$kg{\cdot}m^{-3}$
C_v	effective volumetric heat capacity of the fibrous batting	$kJ{\cdot}m^{-3}{\cdot}K^{-1}$
C_{va}	volumetric heat capacity of the dry air	$kJ{\cdot}m^{-3}{\cdot}K^{-1}$
C_{vf}	effective volumetric heat capacity of the fiber	$kJ{\cdot}m^{-3}{\cdot}K^{-1}$
C_{vw}	volumetric heat capacity of water	$kJ{\cdot}m^{-3}{\cdot}K^{-1}$
D_a	diffusion coefficient of water vapor in the air	$m^2{\cdot}s^{-1}$
d_f	diffusion coefficient of moisture in the fiber	$m^2{\cdot}s^{-1}$
d_l	disperse coefficient of free water in the fibrous batting	$m^2{\cdot}s^{-1}$
E	condensation or evaporation coefficient, dimensionless	
F_L	total thermal radiation incident traveling to the left	W
F_R	total thermal radiation incident traveling to the right	W
h_c	convective mass transfer coefficient	$m{\cdot}s^{-1}$
h_t	convective thermal transfer coefficient	$W{\cdot}m^{-2}{\cdot}K^{-1}$
k	effective thermal conductivity of the fibrous batting	$W{\cdot}m^{-1}{\cdot}K^{-1}$
k_a	thermal conductivity of air	$W{\cdot}m^{-1}{\cdot}K^{-1}$
k_f	thermal conductivity of fiber	$W{\cdot}m^{-1}{\cdot}K^{-1}$
k_w	thermal conductivity of water in the fibrous batting	$W{\cdot}m^{-1}{\cdot}K^{-1}$
K_x	permeability of porous batting	m^2
k_x	coefficient of Darcy's law	$m^2{\cdot}(Pa{\cdot}s)^{-1}$
L	thickness of the fabric batting	m
L_i	thickness of the inner and outer covering fabrics ($i=0$: inner fabric $i=1$: outer fabric)	m
M	molecular weight of the evaporating substance, $M=18.0152$ for water	$g{\cdot}mol^{-1}$
p	pressure of water vapor in the inter-fiber void	Pa
p_{sat}	saturated water vapor pressure at temperature T_s	Pa
p_v	vapor pressure in vapor region at T_v	Pa
R	the universal gas constant, $R=8.314471\times10^7$	$J{\cdot}K^{-1}{\cdot}mol^{-1}$
R_f	radius of fibers	m
R_{ti}	resistance to heat transfer of inner or outer covering fabric (i.e., $i=0$: inner fabric, $i=1$: outer fabric)	$K{\cdot}m^2{\cdot}W^{-1}$
R_{wi}	resistance to water vapor (i.e., $i=0$: inner fabric, $i=1$: outer fabric)	$s{\cdot}m^{-1}$
r	radial distance	m
RH_i	relative humidity of the surroundings (i.e., $i=0$: surface next to human body, $i=1$: surrounding air)	%
Rhf	relative humidity of the air space within the porous batting	%
T	temperature	K
T_i	temperature of the boundaries (i.e., $i=0$: surface next to human body, $i=1$: surrounding air)	K
T_s	temperature at the interface of condensates and vapor	K
T_v	temperature in the vapor region	K
t	time	s
u	velocity of water vapor	$m{\cdot}s^{-1}$
W	water content of the fibrous batting, which is defined as the weight of water divided by the weight of the dry fibrous batting, and maybe greater than 100%	%
W_{ai}	weight of the ith layer of the batting before placing on the instrument in the cold chamber	g
W_{bi}	weight of the ith layer of the batting before placing on the instrument in the cold chamber	g
W_c	critical level of water content above which the liquid water becomes mobile	%
W_f	water content of the fibers in the porous batting	%
WC_i	water content of the ith layer of the batting	%
x	distance from the inner covering fabric (the warm side)	m

Greek symbols

β	radiative sorption constant of the fibers	m^{-1}
ε	porosity of fiber plus condensates (liquid water, or ices)	
ε'	porosity of the fibrous batting (ε = cubic volume of interfiber space/total cubic volume of batting space)	
λ	latent heat of (de)sorption of fibers or condensation of water vapor	$kJ{\cdot}kg^{-1}$
μ	dynamic viscosity of dry water vapor	$kg{\cdot}m^{-1}{\cdot}s^{-1}$
ρ	density of the fibers	$kg{\cdot}m^{-3}$
ρ_w	density of liquid water or ice	$kg{\cdot}m^{-3}$
σ	Boltzmann constant, $=5.6705\times10^{-8}$	$W{\cdot}K^{-4}{\cdot}m^{-2}$

τ	effective tortuosity of the fibrous batting. The degree of bending or twist of the passage of moisture diffusion due to the bending or twist of fibers in the fibrous insulation. It normally changes between 1.0 and 1.2, depending on the fiber arrangements	Γ	total rate of (de)sorption, condensation, freezing and/or evaporation ..... $kg{\cdot}s^{-1}{\cdot}m^{-3}$
ζ_f	fiber emissivity	Γ_{ce}	rate of condensation, freezing and/or evaporation ..... $kg{\cdot}s^{-1}{\cdot}m^{-3}$
ζ_i	surface emissivity of the inner and outer covering fabrics ($i = 1$: inner fabric; $i = 2$: outer fabric)	Γ_{sce}	condensation or evaporation rate per unit surface area of fiber covered with condensates ..... $kg{\cdot}s^{-1}{\cdot}m^{-2}$
		Γ_s	rate of (de)sorption ..... $kg{\cdot}s^{-1}{\cdot}m^{-3}$

and moisture in textiles. They considered the effect of moisture (de)sorption and the associated humidity-dependent air permeability, effect of order of clothing layers, effect of wicking, and the effect of the air permeability of outer fabrics in windy conditions. However, Gibson and Charmchi's models did not consider the radiative heat transfer and moisture bulk flow, which are important transport mechanisms in cold weather conditions. Ghali et al. [13,14] experimentally investigated and theoretical modeled the effect of air penetration through the fabric and fabric motion (simulating the ventilation created by "walking motion"). Ghali et al. [13,14] were the first who did not assume local thermal equilibrium in the biber, which is important in modeling the transient process of ventilation. Ghali et al. [15] also modeled and experimentally investigated the heat and moisture transfer during wicking along the fabric plane.

Fan et al. [16] first introduced dynamic moisture absorption process and radiative heat transfer as well as the movement of liquid condensates [17] in their transient models. The model [17] however was not examined by experiments. With the experimental results, the present work revealed that the previous model should be improved to consider the moisture bulk flow induced by the vapor pressure gradients. In this paper, the improved model is described, numerical simulation has been performed to better understand the effect of moisture movement induced by the partial water vapor pressure, moisture diffusion, condensation, evaporation, and liquid water movement on the distribution of water content and heat loss, and its results are compared with the experimental ones.

2. Model formulation

The model considers a clothing ensemble system, consisting of a thick porous fibrous batting (~10 mm) sandwiched by one thin inner fabric (~0.1 mm) next to the human skin and the other layer of fabric (~0.1 mm) next to the cold environment. The schematic diagram is shown in Fig. 1. Since the fibrous batting is highly porous and the temperature difference between the human skin and the environment is great, radiative heat transfer within the fibrous batting is considered as important.

In forming the mathematical model, we assume that

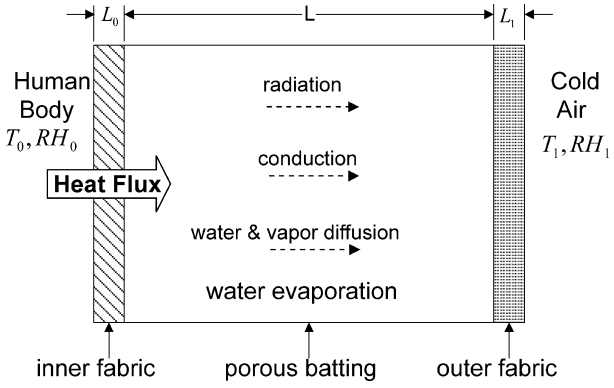

Fig. 1. Schematic diagram of the porous clothing ensemble system.

(1) The porous fibrous batting is isotropic in fiber arrangement and material properties.
(2) Volume changes of the fibers due to changing moisture and water content are neglected.
(3) Local thermal equilibrium exists among all phases and as a consequence, only sublimation or ablimation is considered in the frozen region.
(4) The moisture content at the fiber surface is in sorptive equilibrium with that of the surrounding air.

In this paper, it is believed that moisture bulk flow is induced as a result of the gradient of partial water vapor pressure as in the case of wood drying [18]. The speed of the movement of moist air is modeled by the Darcy's law:

$$u = -\frac{K_x}{\mu}\frac{\partial p}{\partial x} \tag{1}$$

where p is the pressure of water vapor in the inter-fiber void, calculated by

$$p = p_{\text{sat}} \cdot Rhf$$

Based on the conservation of heat energy and applying the two-flux model of radiative heat transfer [16,17,19], at position x and time t, we obtain the heat transfer equation

$$C_v(x,t)\frac{\partial T}{\partial t} = -\varepsilon u C_{va}(x,t)\frac{\partial T}{\partial x} + \frac{\partial}{\partial x}\left(k(x,t)\frac{\partial T}{\partial x}\right) - \frac{\partial F_R}{\partial x} + \frac{\partial F_L}{\partial x} + \lambda(x,t)\Gamma(x,t) \tag{2}$$

where

$$\frac{\partial F_L}{\partial x} = \beta(x)F_L - \beta(x)\sigma T^4(x,t) \tag{3}$$

$$\frac{\partial F_R}{\partial x} = -\beta(x)F_R + \beta(x)\sigma T^4(x,t) \tag{4}$$

where, the effective thermal conductivity $k(x,t)$ is a volumetric average calculated by $k(x,t) = \varepsilon k_a + (1-\varepsilon)(k_f + \frac{\rho}{\rho_w} W k_w)/(1 + \frac{\rho}{\rho_w} W)$, the effective volumetric heat capacity of the fibrous batting is calculated by $C_v = \varepsilon C_{va} + (1-\varepsilon)(C_{vf} + \frac{\rho}{\rho_w} W C_{vw})/(1 + \frac{\rho}{\rho_w} W)$, and the porosity of fiber plus condensates (liquid water, or ice) is calculated by $\varepsilon = \varepsilon' - \frac{\rho}{\rho_w} W(1-\varepsilon')$.

According to mass conservation, water vapor transfer in the inter-fiber void is controlled by the moisture transfer equation:

$$\varepsilon \frac{\partial C_a}{\partial t} = -\varepsilon u \frac{\partial C_a}{\partial x} + \frac{D_a \varepsilon}{\tau} \frac{\partial^2 C_a}{\partial x^2} - \Gamma(x,t) \tag{5}$$

Even when there is no condensation on the surface of a fiber in the porous batting (i.e., the relative humidity is less than 100%), fibers absorb or desorb moisture, the absorption or desorption rate is of the form:

$$\Gamma_s(x,t) = \rho(1-\varepsilon)\frac{\partial C_f(x,t)}{\partial t} \tag{6}$$

where $C_f(x,t)$ is the moisture content within the fiber, which can be integrated by [11]

$$C_f(x,t) = \left\{2/\left(\rho R_f^2\right)\right\} \int_0^{R_f} C'_f r \,\mathrm{d}r \tag{7}$$

where R_f is the radius of the fiber. C'_f is the volumetric moisture concentration in the fiber, which can be determined by the Fickian diffusion law [16]

$$\frac{\partial C'_f}{\partial t} = \frac{1}{r}\frac{\partial}{\partial r}\left(d_f \frac{\partial C'_f}{\partial r}\right) \tag{8}$$

When the relative humidity reaches 100%, condensation or freezing occurs in addition to absorption. Many previous models [3,5,9,17] assumed that extra moisture in the air is condensed instantaneously so that the maximum relative humidity in the air is 100%. This is considered as less appropriate and the cause of some discrepancies between the numerical results of the previous models and experimental results. It is now believed that there is a temporary supersaturation state or ($C_a > C_a^*$ or $Rhf \geqslant 1.0$), i.e., the moisture concentration in the air exceeding the saturated moisture concentration, time is required for the condensation to take place although, given sufficient time, the extra moisture in the air will condense until the moisture concentration in the air reduces to the saturated moisture concentration. On the other hand, when the humidity of surrounding air is below 100%, evaporation or sublimation occurs if there is free water or ice on the fiber surface.

Water condensation and evaporation are modeled using the Hertz–Knudsen equation [20]. The condensation or evaporation rate per unit surface area of fiber covered with condensates (liquid water or ice) is

$$\Gamma_{\mathrm{sce}}(x,t) = -E\sqrt{M/2\pi R}\left(P_{\mathrm{sat}}/\sqrt{T_s} - P_v/\sqrt{T_v}\right) \tag{9}$$

From Eq. (9), we can get [17]

$$\Gamma_{\mathrm{sce}}(x,t) = -E\sqrt{M/2\pi R}(1 - Rhf)P_{\mathrm{sat}}/\sqrt{T} \tag{10}$$

Since the surface area of the fiber covered by condensates in the control volume is $\frac{2\sqrt{(1-\varepsilon')(1-\varepsilon)}}{R_f}$. Therefore, the condensation or evaporation rate per unit volume is

$$\Gamma_{ce}(x,t) = -\frac{2E\sqrt{(1-\varepsilon')(1-\varepsilon)}}{R_f} \times \sqrt{M/2\pi R}(1 - Rhf)P_{\mathrm{sat}}/\sqrt{T} \tag{11}$$

Therefore, the total water accumulation rate $\Gamma(x,t)$ is

$$\Gamma = \Gamma_s + \Gamma_{ce} \tag{12}$$

The free water, i.e., the water on the fiber surface, may diffuse when the free water is in liquid form and its content exceeds a critical value, according to the mass conservation, we have

$$\rho(1-\varepsilon)\frac{\partial \widetilde{W}}{\partial t} = \rho(1-\varepsilon)d_l \frac{\partial^2 \widetilde{W}}{\partial x^2} + \Gamma_{ce}(x,t) \tag{13}$$

where $\widetilde{W} = W(x,t) - W_f(x,t)$ is the free water content. $W_f(x,t) = C_f(x,t)/\rho$ is the water absorbed within the fiber; $W(x,t) = \frac{1}{\rho(1-\varepsilon)}\int_0^t \Gamma(x,t)\,\mathrm{d}t$ is the total water content including that absorbed by the fibers and on the fiber surface.

d_l is defined phenomenologically, and depends on water content, temperature and properties of the fiber batting. $d_l = 0$ when the condensate is immobile, which is the case when the water content is less than a critical value W_c, or when the free water is frozen.

According to energy and mass conservation law, at the boundaries of the fibrous batting, the radiative and conductive heat flow in the batting should be equal to the total heat flow through the covering fabrics. Therefore we can have the following boundary conditions for the main differential equation (2):

$$F_L - F_R + k(0,t)\frac{\partial T}{\partial x}\Big|_{x=0} = \frac{1}{R_{t0}}(T|_{x=0} - T_0) \tag{14}$$

$$F_L - F_R + k(L,t)\frac{\partial T}{\partial x}\Big|_{x=L} = \frac{T_1 - T|_{x=L}}{R_{t1} + (1/h_t)} \tag{15}$$

According to the mass conservation, we can also have the following boundary conditions for Eq. (5):

$$\frac{D_a \varepsilon}{\tau}\frac{\partial C_a}{\partial x}\Big|_{x=0} = \frac{C_a|_{x=0} - C_{a_0}}{R_{w0}} \tag{16}$$

$$\frac{D_a \varepsilon}{\tau}\frac{\partial C_a}{\partial x}\Big|_{x=L} = \frac{C_{a_1} - C_a|_{x=L}}{R_{w1} + (1/h_c)} \tag{17}$$

Considering the radiative heat transfer at the interface between the inner thin fabric and the fibrous batting and that

between the outer thin fabric and the fibrous batting, we have initial conditions for Eqs. (3) and (4) as following

$$(1-\zeta_1)F_L(0,t)+\zeta_1\sigma T^4(0,t)=F_R(0,t) \tag{18}$$

$$(1-\zeta_2)F_R(L,t)+\zeta_2\sigma T^4(L,t)=F_L(L,t) \tag{19}$$

3. Numerical computation

The differential equations in the above section were solved by the Implicit Finite Difference Method, with assumed initial conditions simulating different practical circumstances. The computational procedure was such that, at each time step and each position, the computed vapor concentration $C_a(x,t)$ is compared with the saturation vapor concentration $C_a^*(T(x,t))$ at the corresponding temperature. If the calculated vapor concentration is greater than, or equal to, the saturation one (i.e., $Rhf \geqslant 1.0$), condensation takes place. Otherwise, evaporation or sublimation occurs. In the condensation region, if the temperature is above 0 °C, it is a wet region; if the temperature is below 0 °C, it is a freezing region. The condensation or evaporation rate is calculated by Eq. (11). At each time step and position, the calculated water content W is also compared with the critical water content W_c, under which no liquid water diffusion takes place. If $W > W_c$, Eq. (13) is used to calculate the free water diffusion.

In the numerical computation, the initial condition is 20 °C and 65% RH, the skin temperature is 35 °C, the humidity is 95% RH. The air in a cold chamber is −20 °C and 95% RH. The effect of air velocity is described by h_c. This is the condition under which the fibrous battings are conditioned before testing. In addition to the standard parameters (listed in Table 1) that can be found from the handbooks, actually measured values of the parameters of fibrous battings and covering fabrics are used in the numerical computation except for the critical water content W_c, which depends on the porosity and the surface tension of the fibers. Without accurate measurement, W_c is assumed to be 5% with reference to [16].

4. Brief introduction of experiment

Experiments had been conducted using the instrument shown in Fig. 2. The device has a shallow water container 1 with a porous plate 3 at the top. The container is covered by a manmade skin 2 made of a waterproof, but moisture permeable breathable fabric. The edge of the breathable fabric is sealed with the container so that there is no water leakage. Water is supplied to the container from a water tank 16 through an insulated pipe 14. The water in the water tank is pre-heated to 35 °C. The water level at the water tank is checked frequently to ensure it is higher than the manmade skin so that water is in full contact with the manmade skin at the top of the container. The water temperature in the container 1 is controlled at 35 °C, simulating the human skin temperature. To prevent heat loss from the directions other than the upper right direction, the water container is surrounded with a guard with heating element 13. The temperature of the guard is controlled so that its difference from that of the bottom of the container is less than 0.2 °C. The whole device is further covered by thick insulation foam. The temperature measurement and control are achieved using a computer control system.

In our experiment, 15 plies of viscose batting sandwiched by an inner and outer layer of thin covering nylon fabrics, were tested on the above instrument in a cold chamber of -20 ± 1 °C and $90 \pm 5\%$ *RH*. The properties of the nylon lining fabric and viscose batting are listed in Tables 2 and 3, respectively. Each ply of the battings was conditioned in an air-conditioned room of 20 ± 1 °C and $65 \pm 5\%$ *RH* and weighed using an electronic balance. The accuracy of the digital balance is 0.01 g. The net moisture weight of the batting is 0.1–4.0 g. The order of magnitude of the changes in the weights of the batting relative to the scale accuracy is 10–400. After placing the samples on the instrument in a cold chamber for a pre-determined time, each layer of the battings was re-weighed and the water content of the ith layer is then calculated by

$$WC_i = \frac{W_{ai}-W_{bi}}{W_{bi}} \times 100\% \tag{20}$$

Table 1
Parameters used in the calculation

ρ_{ice}	λ			h_c	k_a	k_f	k_w
	Dry region	Wet region	Freezing region				
920.0	2522.0	2260.0	2593.0	2.294×10^{-3}	0.025	0.1	0.57
τ	h_t	D_a	R_f	R	C_{va}	C_{vf}	C_{vw}
1.05	4.05	2.5×10^{-5}	1.03×10^{-5}	8.314471×10^7	1.169	1300.0	4200.0
W_c	ζ_1	ζ_2	σ	RH_0	RH_1	T_0	T_1
0.5	0.9	0.9	5.672×10^{-8}	99%	90%	306	253

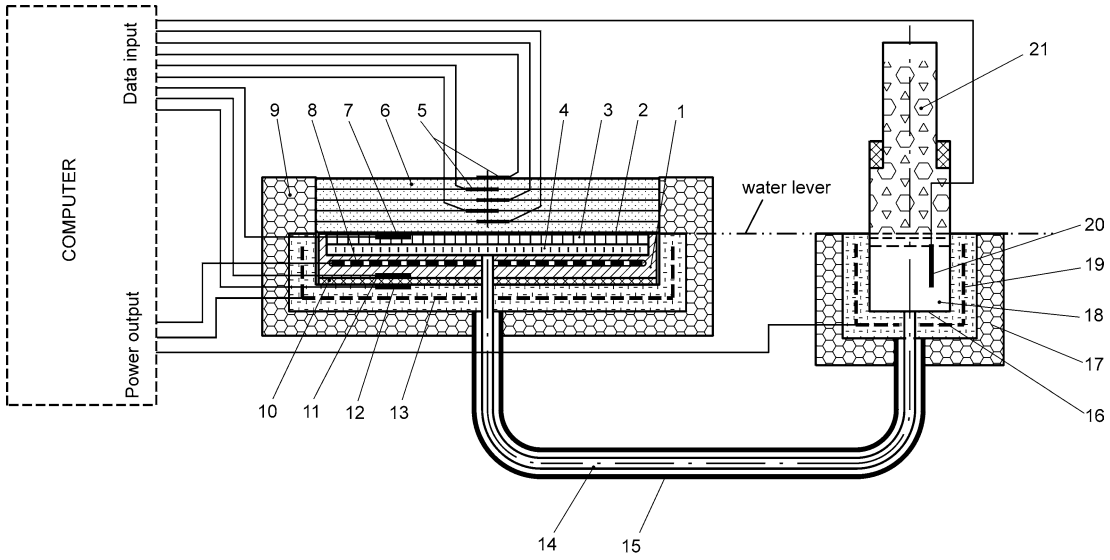

Fig. 2. Schematic design of the instrument.

Table 2
Properties of inner and outer covering fabric

Composition	Nylon
Weave	Woven
Mass [kg·m^{-2}]	0.108
Thickness [m]	2.73×10^{-4}
Resistance to heat transfer ($R_{t0} = R_{t1}$) [K·m^2·W^{-1}]	3.15×10^{-2}
Resistance to water vapor transfer ($R_{w0} = R_{w1}$) [s·m^{-1}]	64.99
Resistance to air penetration [kPa·s·m^{-1}]	0.524
Coefficient of Darcy's law ($\frac{K_x}{\mu}$) [m^2·(Pa·s)$^{-1}$]	5.21×10^{-7}

Table 3
Properties of fibrous battings

Composition	Viscose
Mass [kg·m^{-2}]	0.145
Thickness of each layer [m]	1.94×10^{-3}
Density of the fiber [kg·m^{-3}]	1.53×10^3
Porosity	0.951
Resistance to air penetration [kPa·s·m^{-1}]	0.062
Coefficients of Darcy's law [m^2·(Pa·s)$^{-1}$]	3.106×10^{-5}

5. Verification of the model

The model reported in this paper is applied to calculate the water content and heat flux through the 15 plies viscose batting sandwiched by 2 layers of a nylon fabric to see whether the moisture movement induced by the partial water vapor pressure, a super saturation state in condensing region, dynamic moisture absorption of fibrous materials, the movement of liquid water, and evaporation of water in the model can better explain the experimental observation [18].

The distribution of water content and heat flux are plotted in Figs. 3, and 4, respectively. As can be seen in Fig. 3, the water content in the inner region (i.e., close to the warm human body) is relatively low due to the fact that the moisture is driven by the partial water vapor pressure to the outer (or cold) region, where it is condensed. The condensed, but unfrozen (liquid) water in the outer region may move back to the inner warm region by liquid water diffusion and get re-evaporated in the inner region. From Fig. 3, we can see that, after 24 hours, the predicted water content in outer region (195.92%) is about eight time of that in the inner region (23.27%). Fig. 4 shows that the calculated conductive heat flux through the clothing ensemble system. The conductive heat flux through the clothing ensemble system is calculated by

$$H_{\text{flux}} = \begin{cases} \dfrac{T_0 - T|_{x=0}^{t=n+1}}{r_0} \\ \quad 0 \leqslant x \leqslant L_0 \\ k|_{x=n}^{t=n+1} \dfrac{T|_{x=n}^{t=n+1} - T|_{x=n+1}^{t=n+1}}{x} \\ \quad L_0 \leqslant x \leqslant L_0 + L \\ \dfrac{T_1 - T|_{x=L}^{t=n+1}}{r_1 + (1/h_t)} \\ \quad L_0 + L \leqslant x \leqslant L_0 + L + L_1 \end{cases} \tag{21}$$

As can be seen, it increases fleetly from the inner region to the outer region. This is a result of the transformation of the mainly latent heat transfer (in the form of moisture

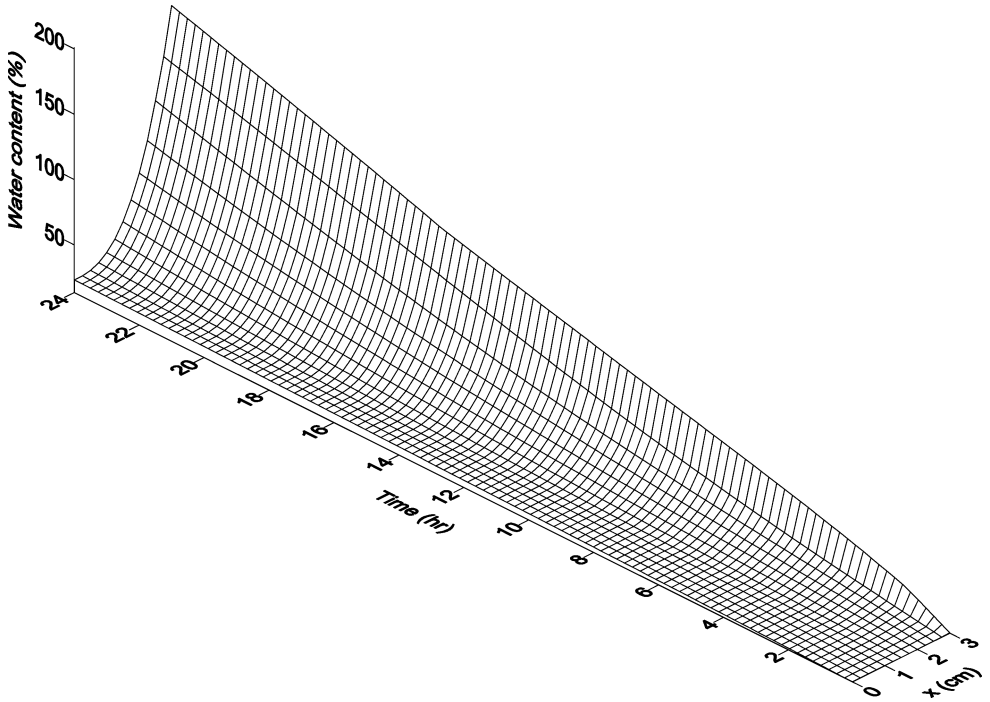

Fig. 3. Change of water content distribution with time in batting (x: distance from the inner covering fabric (warm side)).

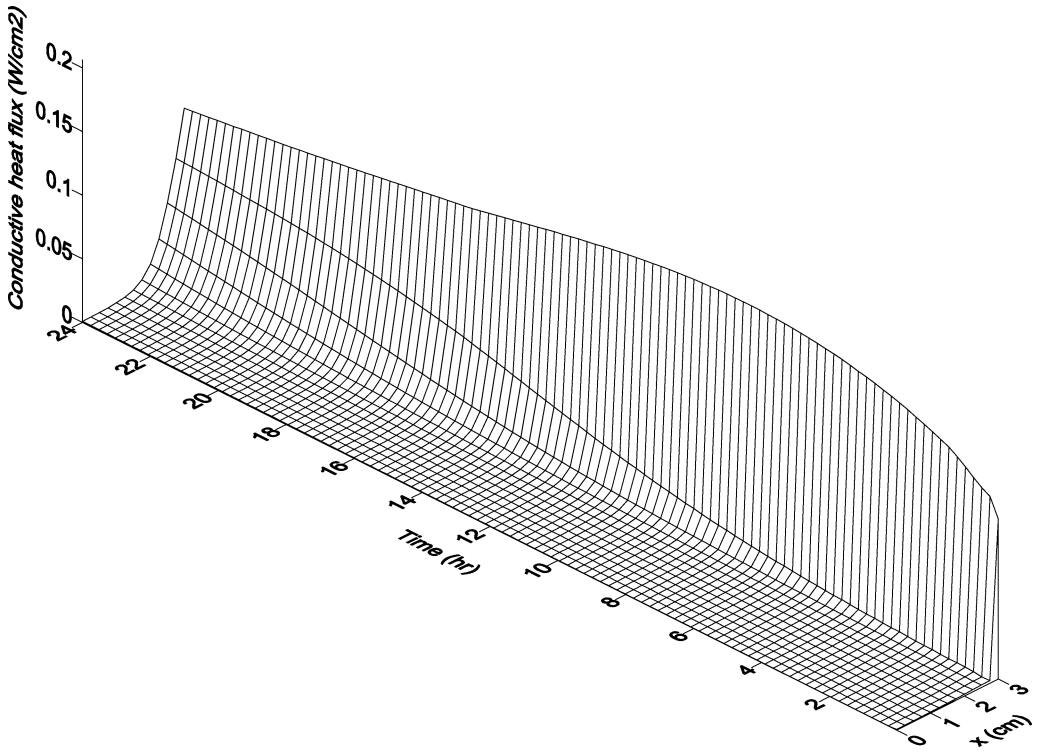

Fig. 4. Distribution of the conductive heat flux through the clothing ensemble system with time (x: distance from the inner covering fabric (warm side)).

movement) in the inner region to the mainly dry heat transfer in the outer region.

The calculated results are in general agreement with our experimental investigation. Fig. 5 compares the numerical and experimental results of water content distribution in fibrous battings. As can be seen, the numerical results fit well with the experimentally measured water content distribution except for the water content after 24 hours in the outer three layers of the battings. The cause of this discrepancy is not fully understood, but may be due to an experimental error in not accounting all the ice condensates at the interface between the outmost layer of the batting and the outer

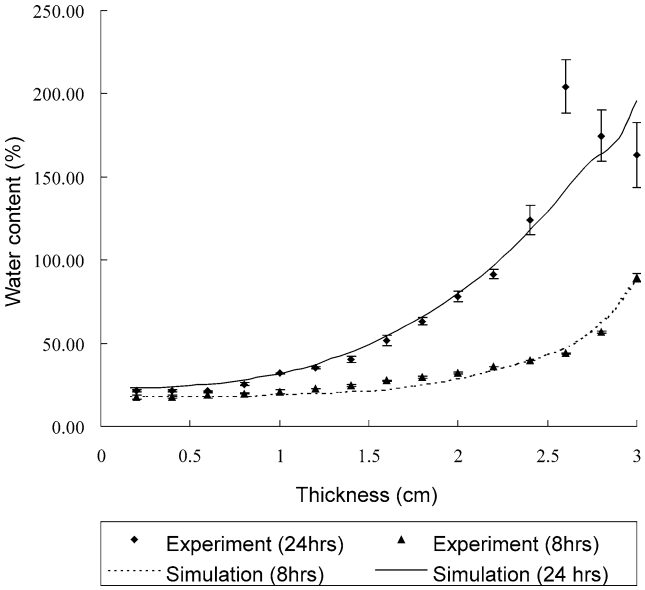

Fig. 5. Comparison of water content distribution between simulation and experiment.

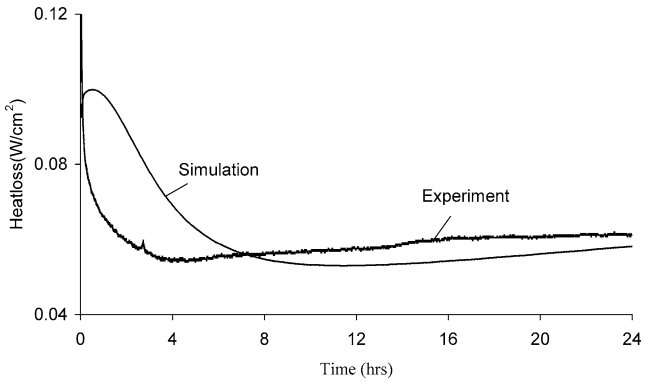

Fig. 6. Comparison of conductive heat loss through the outer nylon fabric between simulation and experiment.

covering fabric as it was observed that, a lot of ice was stick to the outer covering fabric after 24 hours, although little ice was stick to the outer covering fabric after 8 hours testing in the chamber.

Fig. 6 plots the conductive heat loss through the outer nylon fabric from simulation and experiment. The experimental results are calculated from the actually measured temperatures at the two sides of the outer nylon fabric and the theoretical ones are calculated by

$$H_{\text{loss}} = \frac{T_1 - T|_{x=L}}{r_1 + (1/h_t)} \tag{22}$$

As can be seen, the simulation and experimental results agree reasonably well in that the heat flow decreases for several hours and then slowly increases. The initial decrease in heat flow can be explained by the cooling down of the battings in the outer region and the outer fabric as the ambient environment is changed from 20 °C to −20 °C. The gradual increase in heat loss after reaching a minimum is due to the reduction of clothing thermal insulation caused by the accumulation of water in either liquid or ice form as a result of condensation. There is however a discrepancy between the simulation and experimental results in that the experiment showed a faster initial decrease and reached the minimum in about four hours while the simulation has a small initial increase followed by a delayed decrease and takes longer to reach a minimum. The small initial increase and a slowed decrease in the simulation might be caused by the over estimation of the moisture bulk flow according to the Darcy's law near the outer fabric, as a result there is an over estimation of heat transported to the outer region by moisture bulk flow. In actual circumstances, the moisture flow near the outer fabric is influenced by the resistance of the outer fabric, which is not considered in the model.

Table 4
Values of the parameters used in numerical computation

d_l	d_f	E	β
5.4×10^{-11} m^2·s^{-1}	1.512×10^{-16} m^2·s^{-1}	2.4×10^{-4}	250 m^{-1}

6. Simulation results and discussion

The thermal insulation property of fibrous systems is very important to cold protection. In order to optimize the thermal insulation, numerical simulation was performed to better understand the mechanism of heat and mass transfer with moisture absorption, phase change and mobile condensation within the porous fibrous insulation. In each simulation, one parameters listed in Table 4 was changed, but the rest were kept constant as in the table.

6.1. Effect of coefficient of Darcy's law

The effect of the coefficient of Darcy's law $k_x = \frac{K_x}{\mu}$ on the water content distribution is shown in Fig. 7. When $k_x = 0.0$ (i.e., there is no flow of moist air within the fibrous batting. This may be achieved by interlacing the layers of battings with air-impermeable fabrics), the distribution of water content is convex. With the increase of k_x, there is an initial increase in water content in the battings followed by the gradual change of the shape of distribution to concave. The maximum condensation in the battings taken place when k_x is slightly more than zero. This is because, when k_x is zero, moisture is transported only by diffusion and there is not enough moisture supply for condensation in the batting. On the other hand, when $k_x \neq 0.0$, but not too high, enough moisture is supplied by diffusion and bulk flow for condensation over the entire thickness of the battings. When k_x increases further, there will be little condensation in the inner region of the battings due to high moisture bulk flow, but greater condensation at the outer region of the batting. Reduction of k_x can create more even distribution of water content, but total water content in the batting will increase,

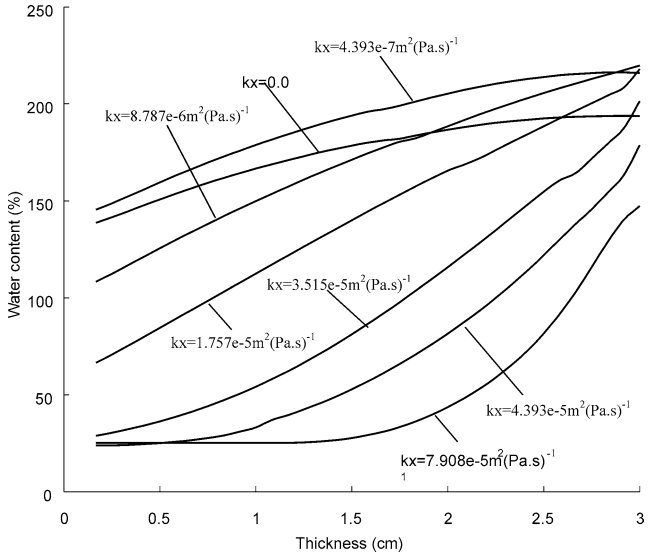

Fig. 7. Water content distribution after 24 hours within battings having different Darcy's law coefficients k_x.

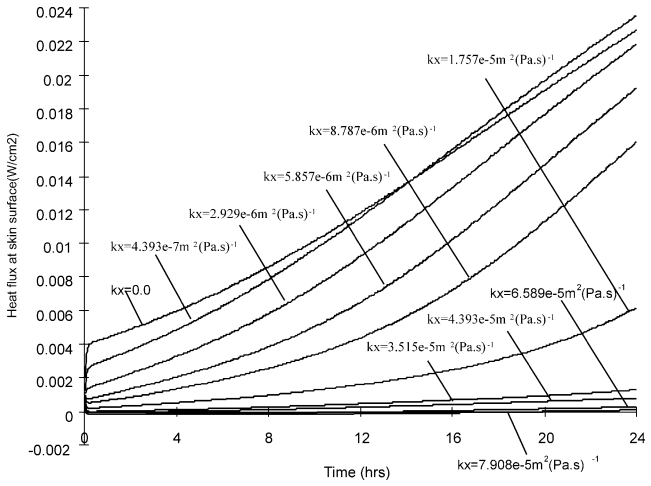

Fig. 8. Heat flux through the inner covering fabric next to skin for battings having different coefficients of Darcy's law k_x.

which is a disadvantage to clothing thermal comfort. Fig. 8 shows the effect of the coefficient of Darcy's law k_x on the conductive heat loss through the inner nylon fabric next to the skin. The heat loss increases with time, since the accumulation of water content in the batting reduces the insulation of the batting. Increased value of k_x tends to reduce the heat flux because the moisture bulk flow reduces the temperature gradient in regions next to skin. Therefore, in general highly porous fibrous batting (with high value of k_x) is advantageous as it minimizes dry heat lost from the skin, minimizes the moisture accumulation and makes a wet region further away from the skin.

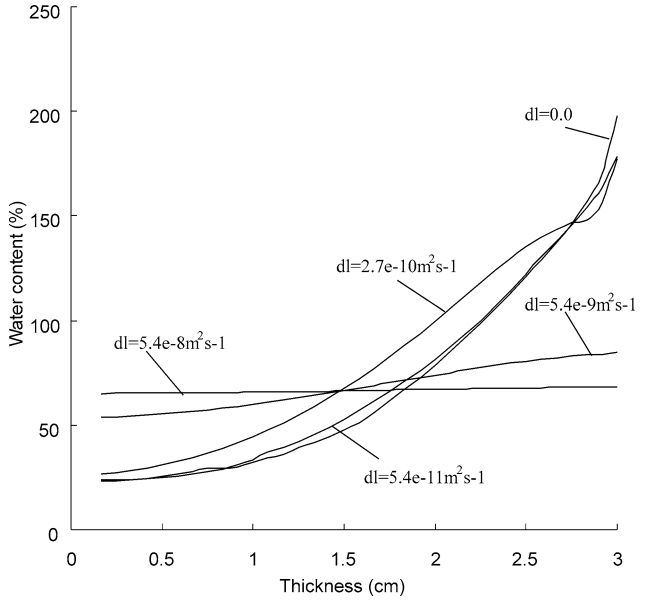

Fig. 9. Water content distribution after 24 hours within battings having different free water disperse coefficient.

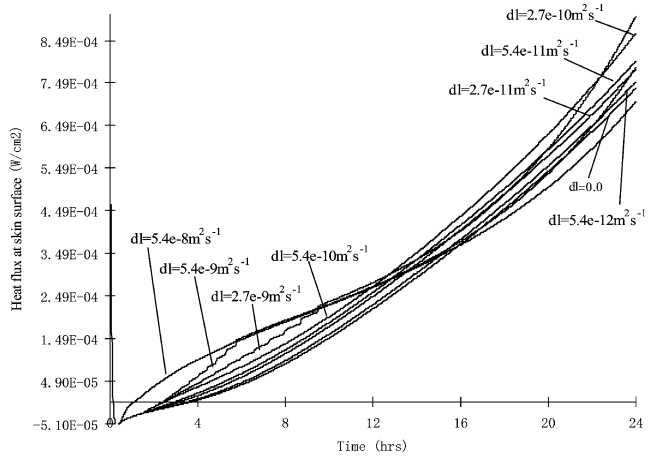

Fig. 10. Heat flux through the inner covering fabric next to skin for battings having different free water disperse coefficient.

6.2. *Effect of disperse coefficient of free water in the fibrous batting d_l*

The effect of disperse coefficient of free water in the fibrous batting d_l on the water content distribution is shown in Fig. 9. When $d_l = 0.0$, there is no movement of liquid water on the fiber surface, the curve of water content distribution is concave, the peak appears at the outermost side of batting. With the increase of d_l, the liquid water overcomes the surface tension and moves to the region having a lower water content when the amount of liquid condensate exceeds a certain critical value. When d_l is equal to or exceeds 5.4×10^{-8} $m^2 \cdot s^{-1}$, the distribution of water content is almost even.

Fig. 10 shows the effect of d_l on heat loss through the inner nylon fabric next to the skin. Generally speaking,

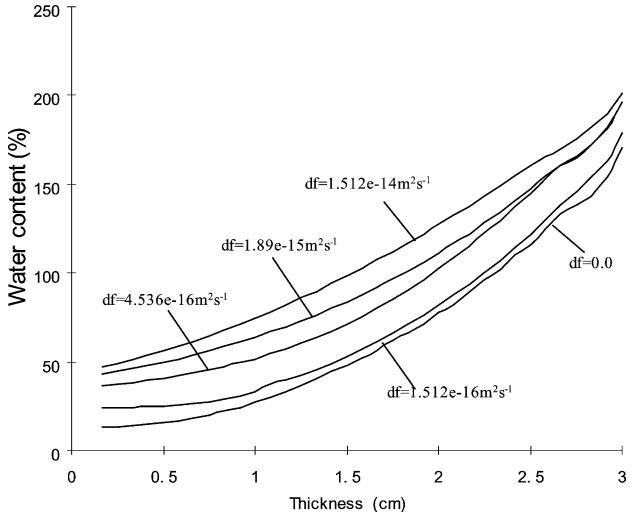

Fig. 11. Water content distribution after 24 hours within battings having different diffusion coefficient of moisture in the fiber after 24 hours.

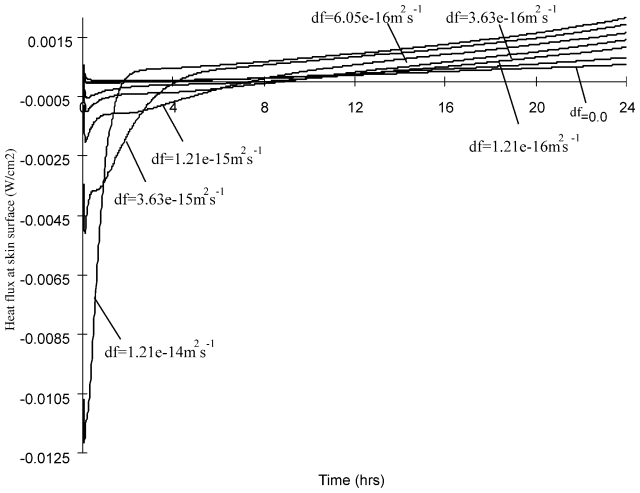

Fig. 12. Heat flux through the inner covering fabric next to skin for battings having different moisture diffusion coefficient.

the effect is relatively small, being less than 10^{-4} W·cm^{-2}. Small amount negative heat flux, viz. heat transfers from the batting to the skin surface, is observed in the initial period of time up to 1 to 4 hours depending on the value of d_l. This negative heat flux is caused by the heat released by moisture absorption and condensation within the batting.

6.3. Effect of diffusion coefficient of moisture in the fiber d_f

The effect of the diffusion coefficient of moisture in the fiber d_f on the water content distribution is shown in Fig. 11. As can be seen, the water content increases with the increase of d_f, but the general pattern of distribution is almost unchanged with the change of d_f.

Fig. 12 shows the effect of d_f on the heat loss through the inner nylon fabric next to the skin. In the initial period, higher d_f results higher negative heat flux due to faster moisture absorption of the fibrous battings and greater amount of heat released. After the initial period, however, higher d_f (corresponding to hygroscopic fibers) will lead to greater heat loss, because water in the batting reduces insulation. The accumulated water in the batting is also a source of "after-chill" discomfort when the wearer stops exercising. From this simulation results, it may be said that hygroscopic fibers may be advantageous for cold protective clothing for short time of exposure, but disadvantageous for clothing for long exposure.

6.4. Effect of condensation or evaporation coefficient E

It may be possible to change the condensation/evaporation coefficient E through the modification of fiber surface. The effect of E on the water content distribution is shown in Fig. 13. The water content increases with the increase of E, but the amount of increase is not even from the inner warm region to the outer cold region. The coefficient E affects

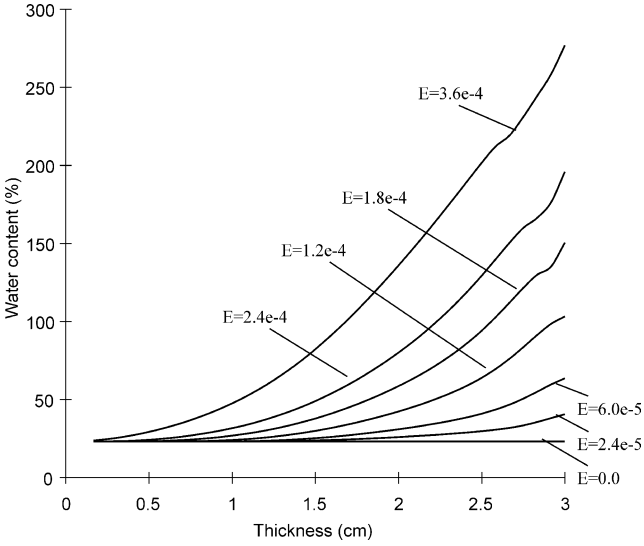

Fig. 13. Water content distribution after 24 hours within battings having different condensation or evaporation coefficient after 24 hours.

mainly the water content in the outer region, where more condensation takes place.

Fig. 14 shows the effect of E on the heat loss through the inner nylon fabric next to the skin. When the value of E is low, there tends to be greater and longer period of negative heat flux as heat released by moisture absorption within the fibrous batting would have higher percentage in the total heat released by moisture absorption and condensation. Generally speaking, greater value of E results in greater amount of heat flux.

6.5. Effect of radiative sorption constant of the fibers β

The effect of radiative sorption constant of the fibers β on the water content distribution is shown in Fig. 15. The water content reduces with the increase of β, but the reduction at

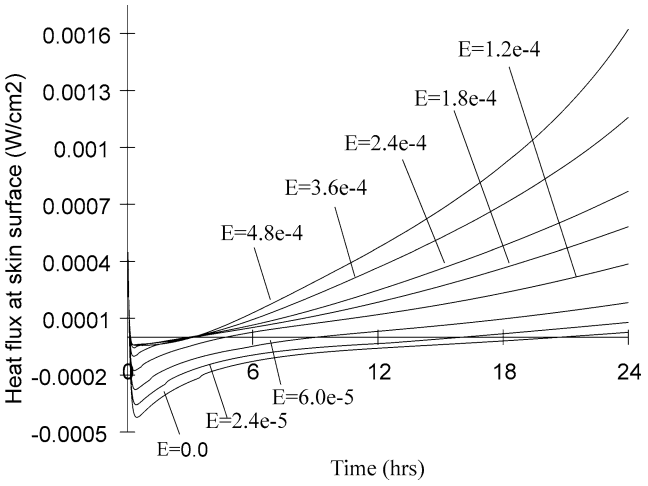

Fig. 14. Heat flux through the inner covering fabric next to skin for different condensation or evaporation coefficient.

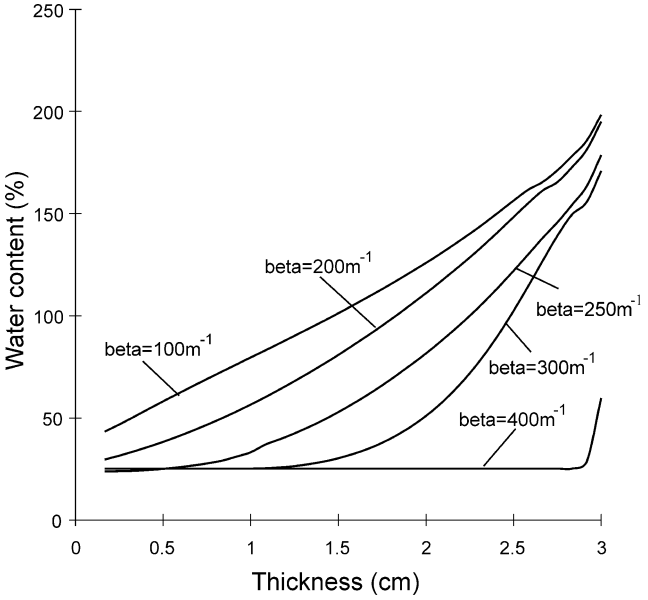

Fig. 15. Water content distribution after 24 hours within battings having different radiative sorption constant of the fibers after 24 hours.

the outermost region is less than that in the inner and middle region.

Fig. 16 shows the effect of β on the heat loss through the inner nylon fabric next to the skin. The heat loss reduces with the increase of β. When β is greater than 300 m^{-1}, the heat flux is negative for very long period of time (over 24 hours), meaning that heat is transferred from the batting to the skin. This is caused by the temperature on the batting side of the inner fabric becomes greater than the skin temperature, arising from radiative heat transfer. From the view of thermal comfort of clothing wearers, a greater value of β may be preferred because it causes less accumulation of water in clothing and less heat loss. The coefficient β is related to

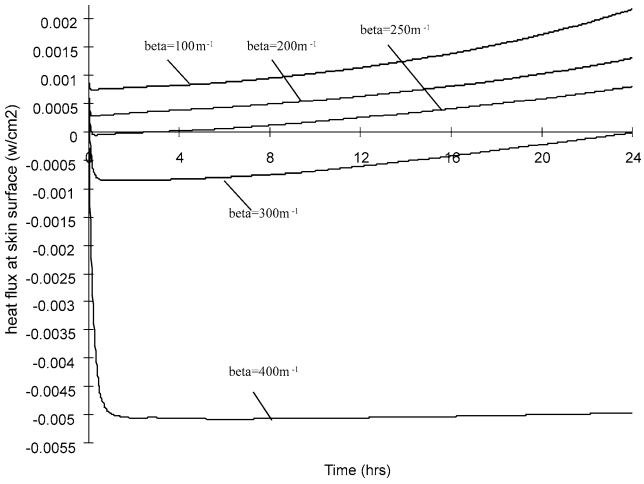

Fig. 16. Heat flux through the inner covering fabric next to skin for battings having different radiative sorption constant of the fibers.

the fractional fiber volume, fiber emissivity and fiber radius [14]:

$$\beta = \frac{(1-\varepsilon)\zeta_f}{R_f} \tag{23}$$

Based on the above relationship, higher fiber content, finer fiber, and greater emissivity of fiber are preferred.

7. Conclusions

In this paper, numerical simulation was reported for an improved model of coupled heat and moisture transfer with phase change and mobile condensates in fibrous insulation. The new model considered the moisture movement induced by the partial water vapor pressure, a super saturation state in condensing region as well as the dynamic moisture absorption of fibrous materials and the movement of liquid condensates. The results of the new model were compared and found in good agreement with the experimental ones.

Based on numerical simulation results, the effect of various material parameters on the heat and moisture transfer are elucidated, optimization of material properties for clothing thermal comfort is contemplated.

It is speculated that higher air permeability of fibrous batting, lower disperse coefficient of free water, lower condensation coefficient and greater radiative sorption constant may be beneficial to thermal comfort during and after excising in the cold weather condition. Hygroscopic fibers with greater value of moisture diffusion coefficient may be advantageous for cold protective clothing for short time of exposure, but disadvantageous for clothing for long exposure.

Acknowledgement

The authors would like to thank the Research Grant Committee of the Hong Kong University Grant Council for funding the project (PolyU 5142/00E).

References

[1] P.S.H. Henry, Diffusion in absorbing media, Proc. Roy. Soc. London Ser. A 171 (1939) 215–241.
[2] Y. Ogniewicz, C.L. Tien, Analysis of condensation in porous insulation, J. Heat Mass Transfer 24 (1981) 421–429.
[3] S. Motakef, M.A. El-Masri, Simultaneous heat and mass transfer with phase change in a porous slab, J. Heat Mass Transfer 29 (1986) 1503–1512.
[4] A.P. Shapiro, S. Motakef, Unsteady heat and mass transfer with phase change in porous slab: Analytical solutions and experimental results, J. Heat Mass Transfer 33 (1990) 163–173.
[5] Y.X. Tao, R.W. Besant, K.S. Rezkallah, Unsteady heat and mass transfer with phase changes in an insulation slab: Frosting effects, Internat. J. Heat Mass Transfer 34 (1991) 1593–1603.
[6] B. Farnworth, A numerical model of the combined diffusion of heat and water vapor through clothing, Tex. Res. J. 56 (1986) 653–665.
[7] K. Vafai, S. Sarkar, Condensation effects in a fibrous insulation slab, J. Heat Transfer 108 (1986) 667–675.
[8] K. Vafai, H.C. Tien, A numerical investigation of phase change effects in porous materials, Internat. J. Heat Mass Transfer 32 (1989) 1261–1277.
[9] Y.X. Tao, R.W. Besant, K.S. Rezkallah, The transient thermal response of a glass-fiber insulation slab with hygroscopic effects, Internat. J. Heat Mass Transfer 35 (1992) 1155–1167.
[10] K. Murata, Heat and mass transfer with condensation in a fibrous insulation slab bounded on one side by a cold surface, Internat. J. Heat Mass Transfer 38 (1995) 3253–3262.
[11] P.W. Gibson, M. Charmchi, Modeling convection/diffusion processes in porous textiles with inclusion of humidity-dependent air permeability, Internat. Comm. Heat Mass Transfer 24 (5) (1997) 709–724.
[12] P.W. Gibson, M. Charmchi, Application of computational fluid dynamics to protective clothing system evaluation, in: Proceedings of the ASME Pressure Vessels and Piping Conference: Computational Technologies for Fluid/Thermal/Structural/Chemical Systems with Industrial Applications, August 1–5 1999, Boston, MA, USA.
[13] K. Ghali, N. Ghaddar, B. Jones, Empirical evaluation of convective heat and moisture transport coefficients in porous cotton medium, J. Heat Transfer 124 (2002) 530–537.
[14] K. Ghali, N. Ghaddar, B. Jones, Modeling of heat and moisture transport by periodic ventilation of thin cotton fibrous media, Internat. J. Heat Mass Transfer 45 (2002) 3703–3714.
[15] K. Ghali, B. Jones, J. Tracy, Modeling heat and mass transfer in fabrics, Internat. J. Heat Mass Transfer 38 (1) (1995) 13–21.
[16] J. Fan, Z. Luo, Y. Li, Heat and moisture transfer with sorption and condensation in porous clothing assemblies and numerical simulation, Internat. J. Heat Mass Transfer 43 (2000) 2989–3000.
[17] J. Fan, X. Wen, Modelling heat and moisture transfer through fibrous insulation with phase change and mobile condensates, Internat. J. Heat Mass Transfer 45 (2002) 4045–4055.
[18] Z. Chen, Primary driving force in wood vacuum drying, Ph.D. Thesis, Virginia Polytechnic Institute and State University, 1997.
[19] B. Farnworth, Mechanics of heat flow through clothing insulation, Tex. Res. J. (1983) 717–725.
[20] E.F. Jones, Evaporation of Water—With Emphasis on Application and Measurements, Lewis Publishers, Michigan, USA, 1992, pp. 25–43.